Immersion freezing efficiencies of ambient particles collected from five different regions across latitudes

Naruki Hiranuma (nhiranuma@wtamu.edu)[1], Brent Auvermann[2], Franco Belosi[3], David Cappelletti[4], Kimberly Cory[1], Manuel Dall'Osto[5], Cory Davis[6], Mauro Mazzola[3], Reece McFarlin[2,7], Joshua Mills[1], Beatrice Moroni[4], Matteo Rinaldi[3], Cheyanne Rodriguez[1], Zachary Salcido[1], Rita Traversi[8], Craig Whiteside[1], Kai Zhang[9]

[1]Department of Life, Earth, and Environmental Science, West Texas A&M University, Canyon, TX, USA, [2]Biological and Agricultural Engineering Department, Texas A&M AgriLife Research, Amarillo, Texas, USA, [3]National Research Council of Italy – Institute of Atmospheric Sciences and Climate (CNR-ISAC), Bologna, Italy, [4]Department of Chemistry, Biology and Biotechnology, University of Perugia, Perugia, Italy, [5]Departament de Biologia Marina i Oceanografia Institut de Ciències del Mar, CSIC Barcelona, Spain, [6]Department of Chemistry and Physics, West Texas A&M University, Canyon, TX, USA, [7]Department of Agricultural Science, West Texas A&M University, Canyon, TX, USA, [8]Department of Chemistry, University of Florence, Florence, Italy, [9]Pacific Northwest National Laboratory, Richland, WA, USA

Motivation

Atmospheric **ice-nucleating particles (INPs)** can influence the formation of clouds, precipitation and Earth's radiation budget (*Boucher et al.*, 2013; *Vergara-Temprado et al.*, 2018). However, our knowledge of INPs – especially their predominant formation through **immersion freezing** (*Hande and Hoose*, 2017) – is scarce due to the **lack of wide spatio-temporal data of INPs across the globe, representing a critical deficiency**. To fill this gap, we started looking into immersion freezing efficiencies of ambient particles collected from different latitudes between 79 °N and 75 °S. We collected particles using single/multi stage aerosol impactors at five different geographic locations, including the Atlantic sector of the Arctic (i, 78.9 °N), an urban location in Europe (ii, 44.5 °N), a rural area in the U.S. (iii, 35.0 °N), a mid-latitude agricultural area in the U.S. (iv, 34.6 °N) and the Antarctica peninsula area around Weddell Sea (v, 71.2 °S), representing unique particle episodes and atmospheric conditions as shown in **Fig. 1**.

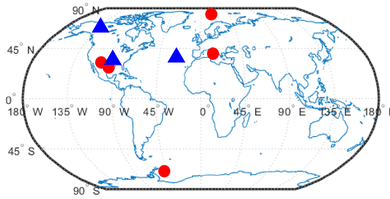

Figure 1. Our sampling locations (red) and future, long-term sampling sites (blue).

Ambient Particle Sampling

Ambient particle samples were collected on 47 mm **Nuclepore**™ filter (Whatman, 0.2 µm pore), **nitrocellulose** membrane (e.g., *Belosi et al.*, 2014) and **aluminum** substrate (*Dall'Osto et al.*, 2017) over the period of January, 2015 – July, 2018. More detailed information, including the sampling dates, Impactor substrate type, flow, ambient particle concentration, inlet (if used), are summarized in **Table 1**.

Table 1. Summary of sampling conditions at five different regions

ID	Location	Date (UTC)	Substrate Type	Flow	Particle Conc.	Inlet
i	Arctic 78°55'03.41" N 11°53'39.61" E 186.4 ft a.s.l.	03/02-03/30/3017; 04/16-05/02/2018	Nuclepore (H_2O_2-pretreated)	7 vlpm	47-195 cm$^{-3, a}$	TSP^f
ii	Urban 44°31'25.03" N 11°20'18.35" E 164.0 ft a.s.l.	10/26-10/31/2017; 02/08-02/12/2018	Nitrocellulose membrane	10 vlpm	6,353-17,401 cm$^{-3, b}$	PM_{10}
iii	Rural [1] 34°58'48.22" N 101°54'50.30" W 3590 ft a.s.l. [2] 35°11'06.18" N 102°05'56.61" W 3849 ft a.s.l.	[1] 04/04/2018; [2] 04/16/2018	Nuclepore (H_2O_2-pretreated)	7 vlpm	<372 µg m$^{-3, c}$	N/A^g
iv	Agricultural Coordinates concealed to protect identity of commercial facilities	07/09-07/11/2017; 07/22-07/24/2018	Nuclepore (H_2O_2-pretreated)	7 vlpm	<2,092 µg m$^{-3, d}$	N/A^g
v	Antarctic ≈71° 11' 16.4394" S 45° 0' 0" W ≈110 ft a.s.l.	01/07-01/18/2015	Aluminum	80 vlpm	TBA^e	N/A^h

a. measure by a combination of SMPS and APS in 2017; *b*. based on CPC measurements in 2017; *c*. measured using a TSI-DustTrak in Busland, TX; *d*. mass measurements using a tapered element oscillating microbalance; *e*. based on TSI3775; *f*. both on the single stage and multistage Dekati® PM10 impactor (DEKATI) sampler - the aerodynamic cut-size of particles on Dekati® >10 µm (stage 1), 10-2.5 µm (stage 2), 2.5-1.0 µm (stage 3), < 1 µm (stage 4) in diameter; *g*. the inlet of a single stage filter holder was exposed to ambient air; *h*. Berner impactor (type LPI80, Hauke) with 50% particle upper cut off points at 0.14, 0.42, 1.2, 3.5 and 10 µm aerodynamic diameter.

Ice Nucleation Experiment

We used an offline droplet-freezing assay instrument, the so-called **West Texas Cryogenic Refrigerator Applied to Freezing Test (WT-CRAFT)** system (*Tobo*, 2016), to measure temperature (*T*)-resolved ice-nucleating particle (INP) concentrations at *T* > -25 °C (with a detection capability of >0.0001 per L of air) for each region (**Fig. 2**). 70 solution droplets (3 µL each) placed on a hydrophobic Vaseline layer were analyzed per experiment. With a cooling rate of 1 °C min^{-1}, **Frozen Fraction** (***FF***) and **ambient INP concentration** (n_{INP}) of super-microliter-sized droplets containing particles suspended from filters were estimated as a function of *T* for every 0.5°C based on the phase transition visually observed in each system. Suspension samples was diluted until we observe their freezing spectrum collapses onto the water background curve.

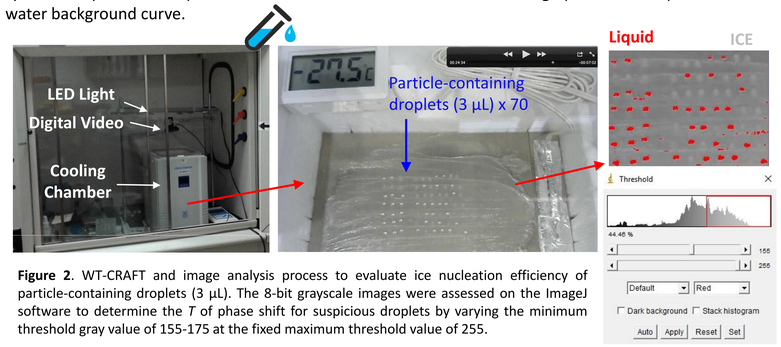

Figure 2. WT-CRAFT and image analysis process to evaluate ice nucleation efficiency of particle-containing droplets (3 µL). The 8-bit grayscale images were assessed on the ImageJ software to determine the *T* of phase shift for suspicious droplets by varying the minimum threshold gray value of 155-175 at the fixed maximum threshold value of 255.

Background Artifact Test

Figure 3 shows our test results of **background freezing levels of field blank samples**. All three substrate types listed in **Table 1** were examined for the *T* down to conceptual homogeneous freezing levels. As seen, **Aluminum** and **Nuclepore** are closely comparable to reference water freezing (i.e., background of WT-CRAFT), and *FF* is insignificant (<6%, freezing of first four drops) above -25 °C. Hence, we decided to characterize our samples on these substrates for *T* down to -25 °C. Note that **nitrocellulose membrane** suffers from artifacts at *T* higher than -25 °C. Less than 6% *FF* is realized only at T of >-22 °C. Hence, we report the results of *T* down to -22 °C for Urban samples. No background corrections were made on our data presented in this study.

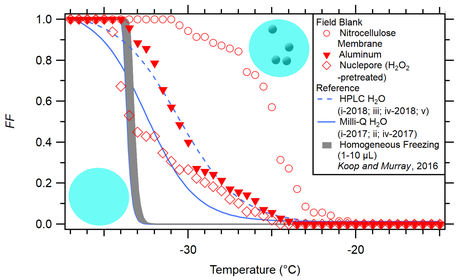

Figure 3. Background freezing spectra of suspensions made using field blank samples (red symbols) in comparison to pure water droplet spectra (lines) as well as theoretical spectra (shaded area, CNT-based).

Parameterization & Results

Our results of **cumulative INP concentrations at -15, -20 and -25 °C from five regions** are summarized in **Fig. 4**. All data are presented in n_{INP} (L^{-1}). The n_{INP} parameterization is well described in *DeMott et al.* (2018). Briefly, we first calculate the INP concentration per volume of liquid, c_{INP}, at a given *T* as:

$$c_{\mathrm{INP}}(T) = -\frac{1}{V_{\mathrm{d}}} ln\left(\frac{N_{\mathrm{u}}(T)}{\mathrm{N}}\right)$$

N_u: # of unfrozen droplets
N: total liquid entity (= 70)
V_d: individual droplet volume (= 3 µL)

Then, we estimate INP concentration per volume of air at given *T* (n_{INP}) as:

$$n_{\mathrm{INP}}(T) = c_{\mathrm{INP}}(T)\left(\frac{V_{\mathrm{w}}}{V_{\mathrm{s}}}\right) \times DF$$

V_w: volume of liquid suspension (L)
V_s: sample volume of air (L)
DF: dilution factor of liquid suspension

Note V_s is scaled to the area of particle-laden air cross section on substrates.

As shown in **Fig. 4**, Our preliminary results show **INP concentrations in polar regions are - as expected - lower compared to mid-latitudes.** The average INP concentrations at -25 °C observed in Ny-Ålesund, Svalbard during May 2015 and June 2016 (= 0.32 ± 0.03 L^{-1}; *Schrod et al.*, 2017) are superposed to guide the eye. Low concentrations of high-latitude INPs have been reported in other previous studies (e.g., *Bigg et al.*, 2001; *Fountain and Ohtake*, 1985; *Mason et al.*, 2015; *Ardon-Dryer and Levin*, 2014; *Belosi et al.*, 2014).

Another important observation is the high variability of mid-latitude INP concentrations. A difference in the aerosol episode and properties may be key for such a high variability in the mid-latitude region. A subset of our WT-CRAFT measurements showed a unique aspect of IN behavior at relatively high *T*s (**Fig. 4 vi**; *T* > -15 °C) in comparison to freezing *T*s of other typical INPs. The reason for **early IN may be biogenic aerosols** (e.g., *Després et al.*, 2012; *Irish et.*, 2017; *Wilson et al.*, 2015), but the quantity of these seems small.

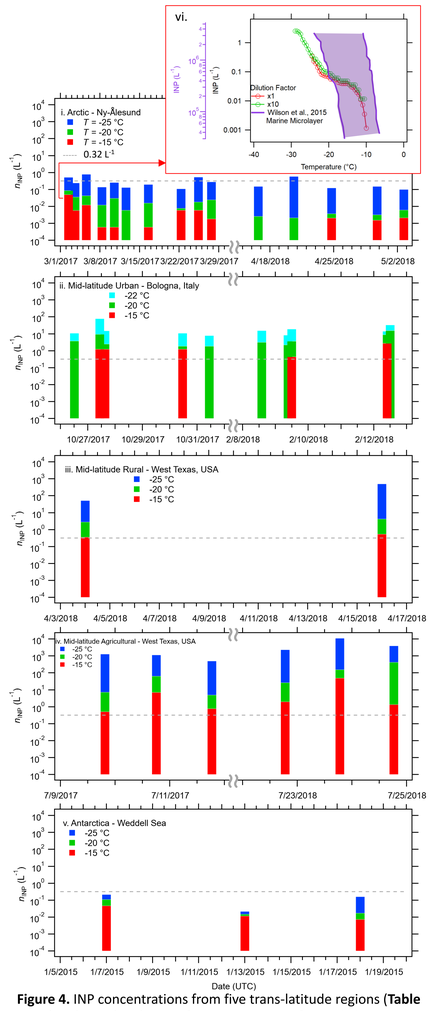

Figure 4. INP concentrations from five trans-latitude regions (**Table 1**). Subpanel vi shows a freezing spectrum from 3/2/2017-.

Future Work: Polar Amplification & INPs

Our polar data suggest **size dependence** and **no notable correlation between ambient aerosol and INP concentrations**, implying certain physicochemical advantages of IN even when the aerosol concentration is low. This indicates the need for further research in **physicochemical properties of INPs and their impact on polar amplification** (*Cohen et al.*, 2014; *Serreze et al.*, 2011).

Figure 5 shows size-segregated INP measurements in the Arctic (Ny-Ålesund) in 2011. The results suggest that the **smallest fraction particles (<1 µm) have the highest IN propensity amongst four sizes**. Correspondingly, only 18% (April 18, 2011) to 35% (April 29, 2011) of INPs had an aerodynamic diameter >1 µm at -25 °C, suggesting the presence of certain physicochemical advantages of IN in submicrometer particles. This number is comparable to two previous size-segregated INP measurements from Alberta, Canada (16% at -12.8 °C; *Vali*, 1966) and the former Soviet Union (37% at -15 to -20 °C; *Berezinski et al.*, 1988).

i. Arctic, Ny-Ålesund

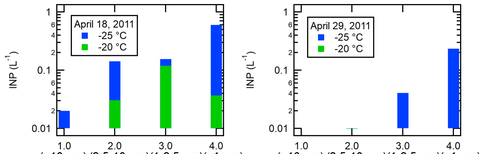

Figure 5. INP number concentrations at droplet freezing *T*s of -20 and -25 ° C (note no measurable data at -15 ° C for these samples).

v. Antarctic, Weddell Sea

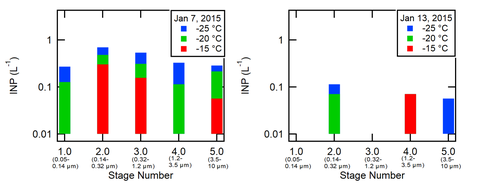

Figure 6. INP number concentrations at droplet freezing *T*s of -15, -20 and -25 ° C.

Figure 6 shows size-segregated INP measurements in the Antarctic (**Fig. 4 v**). In general, the samples from January 7th contained more INPs – an order magnitude higher INPs – compared to January 13th. A cumulative INPs at -25 °C is 2.13 L^{-1} and 0.24 L^{-1} for January 7th and 13th, respectively. **The observed high INPs on the January 7th samples may be due to high aerosol concentration or perhaps indicative of the inclusion of biogenic influence.** We are currently looking into marine biogenic tracer. Our results also suggest that the second smallest fraction particles (0.14-0.32 µm) have the highest IN propensity amongst five sizes. This trends hold true for January 7th and 13th. **Unless the ambient particle size distribution and concentration are responsible for this, chemical composition analyses and physical property characterizations of submicron particles (and vs. supermicron particles) on these samples may be able to shed light on revealing the identity of predominant Antarctic INPs.**

E3SM Modeling Simulation

Our measured INPs in Ny-Ålesund were compared to the **simulated INPs of Energy Exascale Earth System Model (E3SM**, *Zhang et al.*, 2018). Our first test of E3SM model simulation results vs. WT-CRAFT experimental results suggests that CNT overestimates the INP concentration (yet a reasonable agreement within given the model uncertainty) while the D15 parameterization underestimates INPs in this specific location.

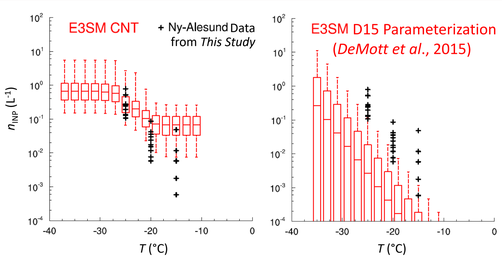

Figure 7. E3SM simulations with CNT (a) and D15 parameterization (b).

Summary

1. **We experimentally elucidated abundance of ambient INPs in five different regions around the world.**
2. **Biogenic aerosols may be responsible for observed high *T* INPs, but their inclusion may be small (maybe one in a million).**
3. **Further investigation in seasonal variation of INP concentrations as well as chemical and biological speciation of ice residuals (on-going!) will enhance the credibility of our experiments.**
4. **More ambient INP measurements and spatio-temporally resolved INP parameterizations are in high demand to optimize the global aerosol-cloud-climate model, including E3SM.**
5. **Such a new series of episode-specific parameterizations might improve the global ice effective radiative forcing uncertainty (± 1.5 W m^{-2}) in the climate model.**

Paul Engler College of Agriculture and Natural Sciences
Dept. of Life, Earth and Environmental Sciences
Discover Real-World Experience

References

Ardon-Dryer & Levin: Atmos. Chem. Phys., 14, 5217-5231, 2014.
Belosi et al.: Atmos. Res., 145-146, 105-111, 2014.
Berezinski et al.: Springer-Germany, 309, 709-712, 1988.
Bigg: Tellus B, 48, 223-233, 1996.
Boucher et al.: Cambridge University Press_UK/USA, 571-657, 2013.
Cohen et al.: Nature Geosci., 7, 627-637, 2014.
Dall'Osto et al.: Sci. Rep., 7, 6047, 2017.
DeMott et al.: Atmos. Chem. Phys., 15, 393-409, 2015.
DeMott et al.: Atmos. Meas. Tech., 11, 6231-6257, 2018.
Després et al.: Tellus Ser. B, 64, 15598, 2012.
Fountain & Ohtake: 1985: Climate Appl. Meteor., 24, 377-382, 1985.
Hande & Hoose.: Atmos. Chem. Phys., 17, 14105-14118, 2017.
Irish et al.: Atmos. Chem. Phys., 17, 10583-10595, 2017.
Koop and Murray: J. Chem. Phys., 145, 211915, 2016.
Schrod, et al.: Geophys. Res. Abs., 19, 13773, 2017.
Mason et al.: Atmos. Chem. Phys., 16, 1637-1651, 2016.
Serreze et al.: Glob. & Planet. Change, 77, 85-96, 2011.
Tobo: Sci. Rep., 6, 32930, 2016.
Vali: Nature, 212, 384-385, 1966.
Vergara-Temprado et al.: Proc. Natl. Acad. Sci. 201721627, 2018.
Wilson et al.: Nature, 525, 234-238, 2015.
Zhang et al.,: 2018: Geosci. Model Dev., 11, 1971-1988, 2018.

Acknowledgements

The authors thank the Japanese Arctic research consortium, ArCS (Arctic Challenge for Sustainability), for the funding support. This material is based upon work supported by the U.S. Department of Energy, Office of Science, Office of Biological and Environmental Research program (Atmospheric Processes) under Award Number DE-FOA-0001761. N. Hiranuma acknowledges the Graduate Office of WTAMU and Ms. Maria Pantazi for financial/partial support.

www.wtamu.edu